Journal of NeuroVirology (2023) 29:400–415
https://doi.org/10.1007/s13365-022-01109-9

Cytomegalovirus infection induces Alzheimer's disease-associated alterations in tau

Prapti H. Mody[1,2] · Kelsey N. Marvin[1] · DiAnna L. Hynds[1] · Laura K. Hanson[1]

Received: 10 August 2022 / Revised: 21 November 2022 / Accepted: 1 December 2022 / Published online: 12 July 2023

Abstract

Alzheimer's disease (AD) manifests with loss of neurons correlated with intercellular deposition of amyloid (amyloid plaques) and intracellular neurofibrillary tangles of hyperphosphorylated tau. However, targeting AD hallmarks has not as yet led to development of an effective treatment despite numerous clinical trials. A better understanding of the early stages of neurodegeneration may lead to development of more effective treatments. One underexplored area is the clinical correlation between infection with herpesviruses and increased risk of AD. We hypothesized that similar to work performed with herpes simplex virus 1 (HSV1), infection with the cytomegalovirus (CMV) herpesvirus increases levels and phosphorylation of tau, similar to AD tauopathy. We used murine CMV (MCMV) to infect mouse fibroblasts and rat neuronal cells to test our hypothesis. MCMV infection increased steady-state levels of primarily high molecular weight forms of tau and altered the patterns of tau phosphorylation. Both changes required viral late gene products. Glycogen synthase kinase 3 beta (GSK3β) was upregulated in the HSVI model, but inhibition with lithium chloride suggested that this enzyme is unlikely to be involved in MCMV infection mediated tau phosphorylation. Thus, we confirm that MCMV, a beta herpes virus, like alpha herpes viruses (e.g., HSV1), can promote tau pathology. This suggests that CMV infection can be useful as another model system to study mechanisms leading to neurodegeneration. Since MCMV infects both mice and rats as permissive hosts, our findings from tissue culture can likely be applied to a variety of AD models to study development of abnormal tau pathology.

Keywords Neurodegeneration · Herpesvirus · Murine cytomegalovirus (MCMV) · Tau hyperphosphorylation · Glycogen synthase kinase 3 (GSK3) · Lithium chloride (LiCl)

Introduction

Alzheimer's disease (AD) is the third leading cause of death for the geriatric population in the USA (NIA 2018). The main symptom of AD is dementia brought about by a gradual loss of neurons concomitant with development of intercellular plaques of amyloid peptides and intracellular accumulation of neurofibrillary tangles of the tau microtubule-binding protein into neurofibrillary tangles (NIA 2018). Amyloid deposition originating from the sequential cleavage of the transmembrane amyloid precursor protein (APP) by β- and γ-secretases is amyloidogenesis specific to AD. Tau tangles are prevalent in many additional neurological conditions including, but not limited to, Pick's disease, traumatic brain injury, aging-related tau astrogliopathy, and chronic traumatic encephalopathy (Kovacs 2017). However, therapies targeting these pathological hallmarks of AD have not been effective at treating the disease, suggesting that treatments targeting earlier pathogenic events in AD progression should be explored. An attractive hypothesis is that co-morbid conditions, like viral infections, contribute to AD onset. Worldwide, herpesvirus infections are rampant, generally affecting 50–100% of the population depending on location and socio-economic status. Cytomegalovirus (CMV) is a beta herpesvirus with high rates of infectivity (up to 80%). Particularly attractive for this work, both alpha (e.g. herpes simplex virus 1 or HSV1) and beta (e.g. CMV) herpesviruses are suggested to alter AD pathology including amyloid production and tau phosphorylation. Of the two clinical hallmarks of AD, tau has a higher correlation with pathology (Bloom 2014; La Joie et al. 2020).

✉ Laura K. Hanson
lhanson@twu.edu

[1] Division of Biology, Texas Woman's University, 304 Administration Drive, Denton, TX 76204, USA

[2] Current affiliation: University of Texas Southwestern Medical Center, Dallas, USA

Tau is a microtubule stabilizing protein expressed at varying levels in different cell types (Avila et al. 2004). It strengthens microtubules in axons for transport of cellular cargo (Avila et al. 2004). There are six isoforms of tau normally expressed in the adult human brain, all of which can be post-translationally altered by phosphorylation and other modifications (Buee 2000). Without modifications, the six isoforms range in size between 35 and 46 kDa (Alonso et al. 2010). Tau isoforms have as many as 80 potential serine/threonine and five tyrosine phosphorylation sites (Buee 2000; Johnson and Stoothoff 2004). Kinases known to phosphorylate tau include glycogen synthase kinase 3 beta (GSK3β), protein kinase A (PKA), and mitogen-activated protein kinase (MAPK). However, the specific roles these kinases play under normal and neurodegenerative conditions are still debated (Liu et al. 2004; Johnson and Stoothoff 2004; Rahman et al. 2006; Carlyle et al. 2014; Ando et al. 2016). In AD, tau proteins are abnormally hyperphosphorylated and dissociate from the microtubules to form neurofibrillary tangles that are not cleared by the proteasome (Kimura et al. 1996). Tau hyperphosphorylation can make the protein more fibrillogenic, and phosphorylation on serines at position 202 and 396 is implicated in AD (Abraha et al. 2000, Haase et al. 2004). This not only interferes with intracellular signaling and trafficking but also leads to a collapse of the cellular cytoskeleton transport mechanisms and neuronal death.

There is clinical correlation between a variety of herpes virus infections and neurodegeneration risk (Letenneur et al. 2008; Lurain et al. 2013; Barnes et al. 2015; Jackson et al. 2017; McQuillan et al. 2018; Hogestyn et al. 2018). DNA from HSV1, herpes simplex virus 2 (HSV2), human cytomegalovirus (HCMV), human herpes virus 6A (HHV6A), HHV6B, and HHV7 can be detected within plaques in AD patient brains (Lin et al. 2002; Kammerman et al. 2006; Readhead et al. 2018). Furthermore, HSV1 can infect central nervous system progenitor cells and, to a lesser extent, mature neurons and astrocytes (Braun et al. 2006). Some researchers have shown that HSV1 directly interacts with APP and is associated with upregulated tau phosphorylation at sites implicated in AD-associated paired helical filaments (Shipley et al. 2005; Wozniak et al. 2009). Current antivirals against HSV1 can reverse this pathology in tissue culture (Wozniak et al. 2011; Powell-Doherty et al. 2020) and treatment correlated with reduced risk of dementia in a retrospective human cohort study (Tzeng et al. 2018).

Cytomegalovirus (CMV) is also widely prevalent in the human population (60–100% depending upon factors such as socio-economic status) that can cause congenital infection (Manicklal et al. 2013). CMV can become latent and reactivate in response to triggers such as stress, aging, or decreased immune surveillance (Cheeran et al. 2009; Manicklal et al. 2013; Jackson et al. 2017). Direct or indirect mechanisms have not yet been reported for CMV and its possible role in neurodegeneration despite a clear association with neuropathogenesis (60–90% children infected in utero show long-term neurological sequelae; Cheeran et al. 2009). CMV infects neural progenitor cells, astrocytes, and immature neurons, among other neuronal cell types (Cheeran et al. 2005, 2009). In addition to a clinical correlation in AD, Lurain et al. (2013) have shown that Aβ42 staining is increased in HCMV-infected human fibroblasts in tissue culture at 6 days after infection (Lurain et al. 2013). We have not identified any studies assessing the relationship between CMV infection and tau regulation.

In the current work, we investigated MCMV-induced changes in tau in NIH3T3 fibroblasts, a model used in the majority of the previous studies. We confirmed very similar tau modifications occurred in the relevant neuronal model, primary cultures of neonatal rat cortical neurons (RCNs). However, in another neuronal model, B35 neuroblastoma cells (Otey et al. 2003), the virally induced modifications of tau were more divergent. We found that MCMV infection (1) increased primarily high-molecular-weight forms of tau, (2) promoted tau phosphorylation at S396 but not S202, and (3) required expression of late viral gene products to induce tau phosphorylation. Interestingly, GSK3β was not upregulated and inhibition of activity had only modest effects on the changes in tau. This result was different than that reported with HSV1 infection. Together, these results suggest that CMV infection may play a role in the dysregulation of tau seen in AD and establish the potential of CMV infection as a model for investigating AD pathogenic mechanisms, both in vitro (as reported here) and in vivo. The numerous rodent models of neurodegeneration, coupled with the ease of CMV infection in rodents, will allow development of sophisticated models investigating the role of herpesvirus infection in AD pathogenesis.

Materials and methods

Cell culture

Murine NIH3T3 fibroblasts (ATCC® CRL-1658™) were maintained on a strict schedule of splitting every 3 days seeding 3×10^5 cells per 75 cm^2 flask. Rat B35 neuroblastoma cells (ATCC® CRL-2754™) were maintained as described by Seifert et al. (2009). Primary rat cortical neurons were isolated from 1-day-old rat pups and maintained in neurobasal media (Gibco-Life Technologies, MD) supplemented with B-27 mitosis inhibitor (Thermo-Fisher Scientific, Waltham, MA) and glutamine (Invitrogen, Waltham, MA) for 14 days before infecting with virus. All experiments involving animals were performed with approval from the TWU Institutional Animal Care and Use Committee in accordance with the Guide for the Care and Use of Laboratory Animals. In

brief, postnatal day 1 Sprague–Dawley rat pups from untimed pregnant dams (Charles River, Wilmington, MA) were cold anesthetized and quickly decapitated. Intact brains were removed from crania and cleared of meninges. Cortices were dissected from coronal slices (~ 1.0 mm), and subcortical white matter was removed. Cortices were dissociated using 2.0 mg/ml papain (Sigma, St. Louis, MO) for 30 min at 37 °C followed by mechanical separation by trituration. RCNs were plated on poly-D-lysine coated six well plates for western blotting.

Viral infection and treatments

The virus used throughout was MCMV Smith strain (ATCC® VR 194). Virus was maintained as previously described (Hanson et al. 1999), and infectious titer was quantified by standard plaque assay on murine NIH3T3 fibroblasts for all experiments. Infections were performed without centrifugal enhancement, but with removal of the inoculum after 1 h incubation. MCMV infections in all cell types were carried out at a multiplicity of infection (MOI) of 2 plaque-forming units per cell (PFU/cell), based upon the titer in NIH3T3 fibroblast cells. Cells were routinely observed for cytopathic effect to infection through a green filter at 10X magnification using a Zeiss light microscope. In some cases, photomicrographs were captured for documentation. The cytopathic response to MCMV infection can vary by cell type, but generally includes cell rounding, syncytia formation, and, in some cell types, alterations in microtubules.

For evaluation of protein expression kinetics, fibroblasts and neuroblastoma cells were seeded onto 60 mm tissue culture dishes at a density of 1×10^6 cells/dish. Twenty-four hours after plating, cells were infected with MCMV at an MOI of 2 PFU/cell, or mock infected by comparable media changes without virus. In order to determine whether the media change itself altered cellular proteins, an uninfected sample of lysates from cells that had no media change was included in all experiments (designated as U throughout). In all cases, the 0 h is the sample collected at the same time as the media change after 1 h, which allowed for viral binding and entry followed by removal of residual unbound virus. Primary RCNs extracted from 1-day-old pup brains were seeded onto 60 mm tissue culture dishes at a similar cell density and allowed to stabilize for 14 days. Half the media was replaced with fresh media (Neurobasal-B27-glutamine; Invitrogen/Fisher, Waltham, MA) every 4 days, and cells were infected with MCMV on day 15 using a MOI of 2 PFU/cell. For all three cell types, lysates were prepared at 0, 12, 24, 48, and 72 h post infection (HPI) by washing twice with sterile phosphate-buffered saline (PBS), applying lysis buffer (50 mM Tris, 1% SDS, pH 7.5) and scraping cells into microfuge tubes for storage until analysis.

For initial mechanistic studies, we inhibited viral DNA replication with phosphonoformic acid (PFA; also known as foscarnet) at a working concentration of 300 µg/ml and GSK3 with 50 mM lithium chloride (LiCl, Sigma Aldrich, St. Louis, MO) at the 0 h of infection (after viral binding) in NIH3T3 fibroblasts. In some experiments, LiCl was added at 24 HPI. Lysates were harvested at 0, 12, 24, 48, and 72 HPI in western lysis buffer to analyze major capsid protein (MCP) expression and at 48 HPI to evaluate how inhibiting GSK3β affected tau phosphorylation. Western blots were performed for viral proteins, tau, phospho-tau S396, and phospho-tau S202. Conditioned media from each sample was used to titer infectious virus by standard plaque assay.

Western blot analysis

Lysates were subjected to western blot analysis as previously described (Hanson et al. 1999), except that total protein content was determined using the DC protein assay kit (Bio-Rad, Hercules, CA) and 20 µg total protein was loaded in each lane, except for some RCN samples where 40 µl total lysate was loaded. Antibodies and conditions used are shown in Table 1. Primary antibodies included anti-α-tubulin (Sigma-Aldrich, St. Louis, MO) and anti-β-actin (Sigma-Aldrich, St. Louis, MO), made in mouse, and anti-tau (Sigma-Aldrich, St. Louis, MO), anti-GSK3β (Sigma-Aldrich, St. Louis, MO), anti-tau-phospho-S202 (Abcam, Waltham, MA), anti-tau-phospho-S396 (Novus, Centennial, CO), anti-early protein (E1; Ciocco-Schmitt et al. 2002), anti-major capsid protein (MCP; Hanson et al. 2009), and anti-m143 (Hanson et al. 2005), made in rabbit (Table 1). The secondary antibodies used were goat anti-rabbit and goat anti-mouse conjugated to either IRDye 800CW or IRDye 680RD (both from Licor, Lincoln, NE; Table 1). Image Studio software (LiCor, Lincoln, NE) was used to quantify density from single bands, and NIH ImageJ software (NIH, Bethesda, MD) was used to analyze multiple tau bands. In both types of analyses, levels were normalized to loading controls (β-actin or α-tubulin) and normalized levels from mock infected samples set at 1. Time points were compared to 0 HPI unless a mock-infected condition at the same time point was included. For phosphorylated tau and total tau, lane profiles were background subtracted using a horizontal baseline at the lowest point and areas under the curve (AUC) for each band were determined. The total amount of tau was calculated by adding the AUC of each band, grouping bands less than 50 kDa (low molecular weight forms) and those migrating at 50 kDa and higher (high molecular weight forms).

Statistical analyses

Two-way repeated measures analysis of variance (ANOVA) was performed followed by Fisher's least significant

Table 1 List of antibodies used for the studies and their use conditions[a]

Antibody	Dilution	Catalog number	Source	Incubation conditions	
				Time	Temperature
Primary antibodies					
Mouse anti-α-tubulin	1:5000	T5168 clone B-5–1-2	Sigma-Aldrich	1 h	RT
Mouse anti-β-actin	1:5000	A1978 clone AC-15	Sigma-Aldrich	1 h	RT
Rabbit anti tau	1:1000	SAB4501826	Sigma-Aldrich	3 h	RT
Rabbit anti-GSK-3β	1:2000	G7914	Sigma-Aldrich	1 h	RT
Rabbit anti-tau phospho-S202	1:1000	Ab198387	Abcam	Overnight	4 °C
Rabbit anti-tau phospho-S396	1:1000	NBP2 67,702	Novus	3 h	RT
Rabbit anti-early protein (E1)	1:1000		Ciocco-Schmitt et al. (2002)	1 h	RT
Rabbit anti-major capsid protein (MCP)	1:1000		Hanson et al. (2009)	1 h	RT
Rabbit anti-m143	1:1000		Hanson et al. (2005)	1 h	RT
Secondary antibodies					
Goat anti rabbit IRDye 800CW	1:15,000	926 32,211	Li-Cor	1 h	RT (dark)
Goat anti mouse IRDye 680RD	1:15,000	926 68,070	Li-Cor	1 h	RT (dark)

[a]All antibody stock solutions were in the range of 0.9 to 1 mg/ml except for E1, MCP, and m143 which were serum from immunized rabbits and G7914, anti-GSK-3β, which was 0.5 mg/ml

difference (LSD) test for comparisons of target protein levels in uninfected and infected cells. For datasets that had samples subjected to infection as well as foscarnet treatment, three-way repeated measures ANOVA was performed followed by Fisher's LSD test. For viral titer comparison between samples in the GSK3 inhibition experiment, one-way ANOVA was performed followed by Fisher's LSD test. All statistical analyses were run in GraphPad Prism software, version 8.1. For all analyses, a p-value of 0.05 was considered to be significant and is indicated in the figures as $*p \leq 0.05$.

Results

Rat B35 neuroblastoma cells and primary RCN are permissive for MCMV

Demonstration of successful MCMV infection in rat neuronal cells was done by analyzing for cytopathic effect, detection of viral early protein 1 (E1), and late protein, i.e., major capsid protein (MCP), and titering infectious virus from conditioned media taken from infected cells. Both B35 rat neuroblastoma cells and rat cortical neurons (RCNs) exhibited cytopathic effect similar to that observed in fibroblasts after MCMV infection (Fig. 1a). All four isoforms of the viral E1 protein were expressed in neuroblastoma cells and RCNs as determined by western blotting (Fig. 1b). Mean titers obtained from MCMV-infected fibroblasts and B35 cells were similar (5×10^6 and 4×10^6 PFU/ml, respectively: Fig. 1b). For the RCNs, the titer was lower, 3×10^4 PFU/ml (Fig. 1b), as reported previously (Braun et al. 2006). MCP was also detected by western blotting in NIH3T3 and B35 cells at 48 HPI, but was below the level of detection in RCNs at this time (Fig. 1c). However, MCP was detected in RCNs by 72 HPI (Fig. 1d). This is not unexpected as primary neurons are not the most permissive brain cell type for herpes viruses. However, the cytopathic effect, along with expression of both early and late proteins, and production of infectious virus, confirmed that MCMV can undergo a complete replication cycle in rat neuronal cells.

MCMV infection increases high molecular weight tau protein levels

HSV-1 infection leads to changes in levels and modifications of tau (Shipley et al. 2005; Wozniak et al. 2009; De Chiara et al. 2019; Powell-Doherty et al. 2020), but it is not known if other herpes viruses can have a similar effect. We used western blotting for total tau to determine whether MCMV infection altered its protein expression patterns (Fig. 2). Compared to uninfected or mock infected cells, tau was increased in response to MCMV infection of murine fibroblasts at late times (48 and 72 HPI; Fig. 2a, b). Because unmodified tau protein isoforms range from 35 to 46 kDa (Buee 2000), we grouped the detected tau bands into low (below 50 kDa) and high (50 to 250 kDa) molecular weight forms. From densitometric quantitation, the increase in tau resulted primarily from changes in high molecular weight forms (50–250 kDa; Fig. 2b).

Western blots for total tau in both rat neuronal cell models showed similar results. In B35 cells, although less dramatic than the change induced in fibroblasts, the increase was still primarily in high molecular weight tau (Fig. 2c). In RCNs, the change in the protein expression pattern was strikingly

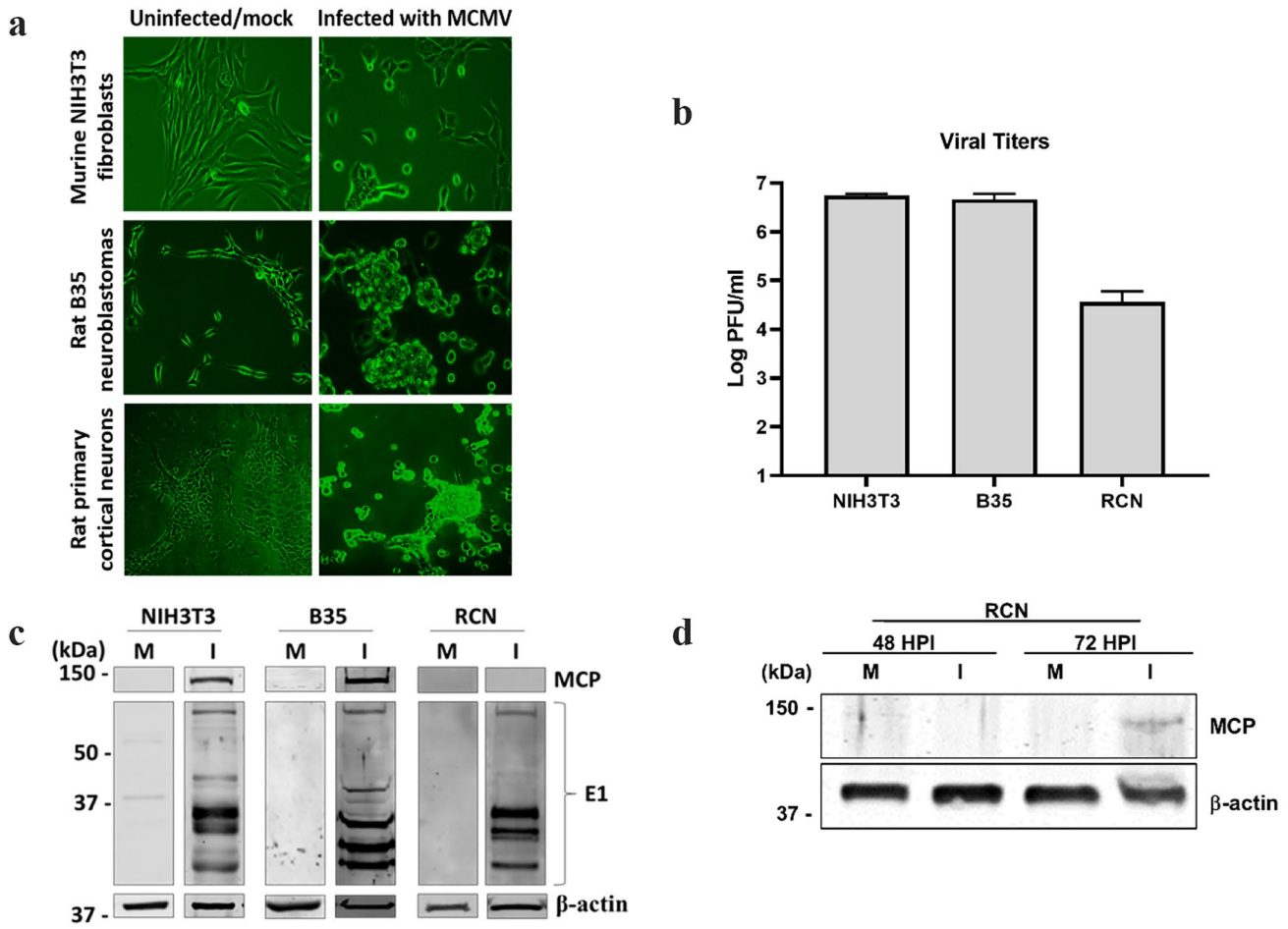

Fig. 1 Rat neuronal cells are permissive for MCMV infection. **a** Photomicrographs showing that murine cytomegalovirus (MCMV) infection at an MOI of 2 PFU/cell resulted in cytopathic effect in NIH3T3 cells (top panel), which has previously been reported (Van Den Pol et al. 2000) and similar cytopathic effect in B35 cells (middle panel) and rat cortical neurons (RCNs; bottom panel). **b** Measurement of viral titers by standard plaque assay 48 h post-infection (HPI) showed that NIH3T3 cells, B35 cells, and RCNs could each support active MCMV infection with viral titers of 5.5×10^6, 4.7×10^6, and 3.7×10^4 plaque-forming units (PFUs)/ml, respectively. Data are means ± SEM from two separate experiments. **c** Representative western blots showing protein levels of the late viral protein major capsid protein (MCP; 120 kDa) and 4 isoforms of viral early protein 1 (E1) with bands at approximately 33, 36, 38, and 87 kDa, as reported previously (Ciocco-Schmitt et al. 2002), from either mock infected (M) or MCMV infected (I) cells. **d** Representative western blots showing that MCP is expressed at levels measurable by western blot analysis by 72 HPI in RCNs, while it is undetectable in MCMV infected RCNs at 48 HPI or in mock (M) infected cells at either time point

similar to that seen for the fibroblasts (Fig. 2d). In all three cell types, a band of around 75 kDa was evident from 12 HPI onward, while additional bands of 150 kDa or higher were detectable by 48 h. These results support the possibility of similar regulation and modifications of tau in the neuronal and fibroblast cells.

Tau phosphorylation at serine 396, but not Serine 202, is increased during MCMV infection

We next investigated whether there is an increase in tau phosphorylated at two sites (S396 and S202) associated with AD and after HSV-1 infection (Kimura et al. 1996; Wozniak et al. 2009). Phosphorylation at these two sites was induced during HSV-1 infection of human neuroblastoma cells; however, the studies were performed only via immunofluorescence at one time point (Wozniak et al. 2009). The increase in HSV-1 induced tau phosphorylated at S396 was confirmed in cultured murine hippocampal neurons, and timing of this particular change was analyzed by western blot analysis, however not compared with levels of total tau or other modifications (Powell-Doherty et al. 2020). We evaluated over the same time course as total tau and analyzed cell lysates by western blotting with antibodies against phospho-tau S396 and S202. There was a clear increase in phosphorylation at S396 (Fig. 3a, b) from 24 HPI through 72 HPI

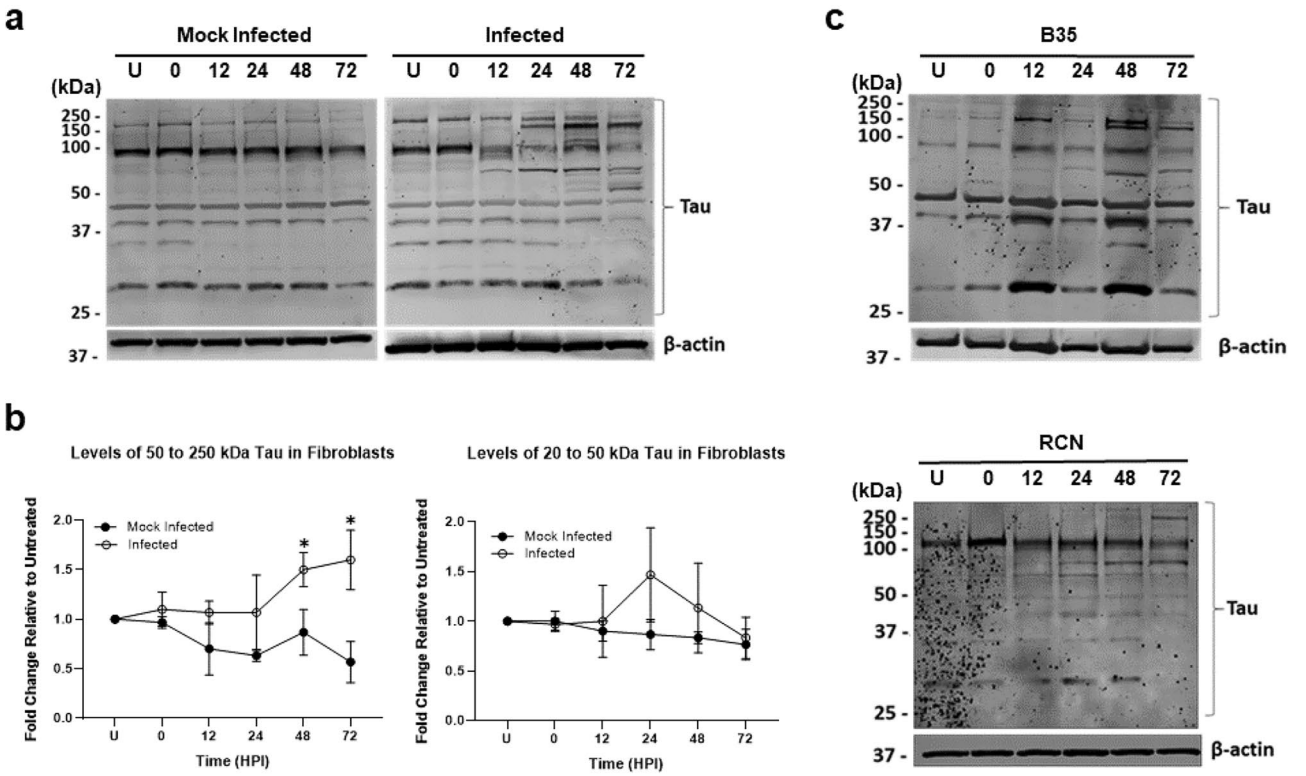

Fig. 2 Total tau is increased during MCMV infection. **a** Representative western blots for total tau in NIH3T3 fibroblasts either untreated (U) or receiving a media change without (mock infected, left blot) or with an MOI of 2 PFU/cell of murine cytomegalovirus (MCMV) for 0 to 72 h showing increases in primarily high molecular weight forms of tau. **b** Scanning densitometry analyses of western blotting for high (50 to 250 kDa) and low (20 to 50 kDa) molecular weight forms of tau in mock infected and infected cells show that MCMV infection significantly increases high molecular weight forms of tau at 48 and 72 h post-infection (HPI). Data are expressed as mean ± SD normalized to β-actin loading controls with the level for untreated cells (U) set to 1.0. Significant differences compared to cells briefly exposed to virus or media change (0 time point) are indicated by $*p \leq 0.05$ (two-way repeated measures ANOVA with Fisher's least significant difference (LSD) post hoc; $n = 3$). **c** Western blots showing similar increased in high molecular weight forms of tau after MCMV infection in rat neuroblastoma B35 cells and primary rat cortical neuron (RCN) cultures

in infected cells. The size of approximately 150 kDa is very consistent with some of the bands detected with the total tau antibody at the same time points.

The uninfected rat B35 cells had a greater variety of tau forms that were phosphorylated at S396 (Fig. 3c). However, as seen with the total tau, a similar high molecular weight phospho-tau (S396) band around the size of 150 kDa became enhanced at 48 and 72 HPI. In uninfected primary RCN, there were 4 predominant bands for tau phosphorylated at S396 in the size range of 70 to 100 kDa. With the progression of MCMV infection, some alterations in the relative intensities of the bands in this size range were observed and additional high molecular weight bands were detectable from 24 HPI onwards (Fig. 3d). Thus, as with the total tau, all three cell types had increased phosphorylation at S396 on high-molecular weight forms of tau.

Considering that tau phosphorylation at serine 202 was also increased during HSV-1 infection (Wozniak et al. 2009), we analyzed whether the same was true for MCMV infection. In fibroblasts, there were more tau bands detected with the anti S202 antibody than the anti S396 antibody to begin with, and there was no difference detected after infection (Fig. 4a, b). Thus, the virus may selectively affect phosphorylation pathways or may be upregulating phosphorylation by kinases targeting specific sites on tau.

Using the same primary antibody, we did not detect phosphorylation of tau at S202 in rat neuroblastomas B35 cells (Fig. 4c). This might be a common characteristic of some neuroblastomas, as human SH-SY5Y cells similarly had low levels of S202 isoforms detected (Boban et al. 2019). The RCNs exhibited a pattern more like that of the NIH3T3 fibroblast cells. There were a number of bands detected with the anti-S202 antibody in the uninfected cells that did not change in band pattern or intensities at 12 or 48 HPI (Fig. 4d). Thus, MCMV likely affects tau phosphorylation in neurons in a manner similar to that in fibroblasts.

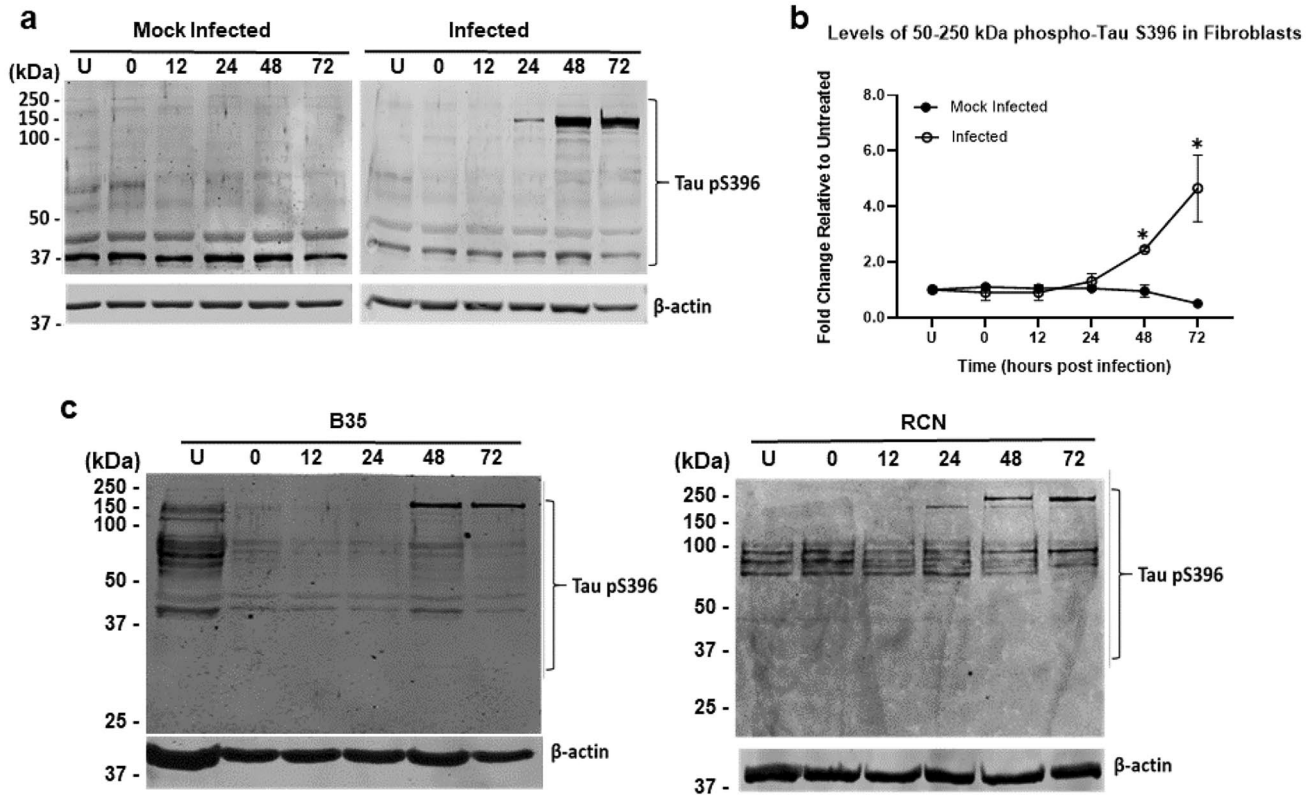

Fig. 3 Phosphorylation of tau at serine 396 is induced during CMV infection. **a** Representative western blots for tau phosphorylated at serine 396 (S396) from NIH3T3 fibroblasts either untreated (U), mock infected (left blot), or infected (right blot) with MCMV for 0 to 72 h showing that increased phosphorylation of S396 is detectable from 24 to 72 h post-infection (HPI). **b** Densitometric analyses of western blots for tau phosphorylated at S396 in mock infected and infected NIH3T3 fibroblasts showing significant increases in high molecular weight forms (50 to 250 kDa) at 48 and 72 HPI, compared to the 0 HPI time point. Data are expressed as means ± SD, normalized for equal loading against β-actin with untreated cultures (U) being set to 1.0. Significant differences compared to the 0 time point are indicated by $*p \leq 0.05$ (two-way repeated measures ANOVA with Fisher's least significant difference (LSD) post hoc; $n = 3$). **c** Western blots for tau phosphorylated at S396 in rat B35 neuroblastoma cells and cultured primary cortical neurons (RCNs) showing increased S396 phosphorylation in high molecular weight immunoreactive bands at 24 to 72 HPI

Viral late gene products are involved in the changes in tau

As the tau alterations were primarily detected at late time points, we used foscarnet to inhibit viral late gene products (Crumpacker 1992) to investigate their importance. Figure 5a shows the controls validating the inhibition of viral late protein, MCP, and expression. The expression of an early viral marker, m143, or of cellular protein β-actin were not affected. In the absence of viral genome replication and late gene products, most of the tau increase was not detected (Fig. 5b, c). In some experiments, the levels of some tau isoforms appeared to be decreased at early times, or in the presence of foscarnet (Fig. 5b). In addition, the approximately 75 kDa form was still detectable from 12 HPI onward. More detailed analysis of specific isoforms or modifications may be warranted in the future to determine whether viral immediate-early or early products may be affecting certain modifications. However, viral genome replication and late gene products are needed for most of the increase in high-molecular weight tau protein levels.

As the increase in phosphorylation at S396 was seen at late time points, we also examined the impact of foscarnet on the phospho-S396 staining patterns. In the absence of viral late proteins, the induced phosphorylation at S396 was not present (Fig. 5c, d). The tau phosphorylation at S396 in mock infected cells remained largely unchanged through 72 HPI, with or without foscarnet treatment (Fig. 5d). Thus, CMV infection induces tau phosphorylation at S396 and viral late gene expression is required for this increase.

MCMV infection does not affect levels of GSK3β

CMV is known to both upregulate phosphatase expression and incorporate host phosphatases in its virion (Hakki and Geballe 2008). Thus, the increase in high-molecular weight forms of tau, including that detected with the anti-Ser396 antibody, is most likely due to altered kinase activity rather than

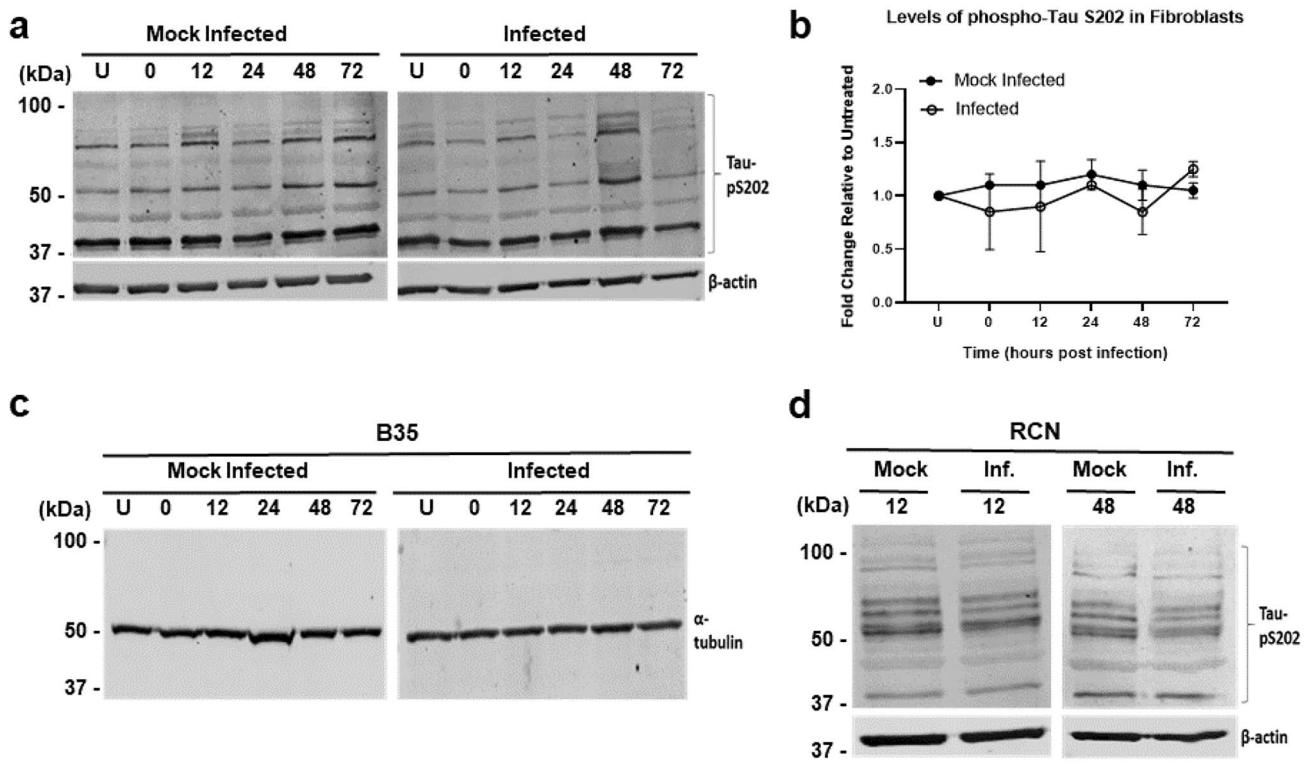

Fig. 4 Tau phosphorylation at S202 remains unaltered during MCMV infection. **a** Representative western blots for tau phosphorylated at serine 202 (S202) from NIH3T3 fibroblasts untreated (U), mock infected (left blot), or infected (right blot) with MCMV for 0 to 72 h showing that S202 phosphorylation did not appreciable change in response to MCMV infection. **b** Scanning densitometric analyses of western blots for tau phosphorylated at S202 in mock infected and infected NIH3T3 fibroblasts confirms that the levels of tau phosphorylated at S202 did not differ with MCMV infection for up to 72 h post-infection (HPI), compared to the 0 HPI time point. Data are expressed as means ± SD, normalized for equal loading against β-actin with untreated (U) cells at 0 h being set to 1.0 ($n = 2$). **c** Representative western blots for tau phosphorylated at S202 from B35 neuroblastoma cells either mock or MCMV infected from 0 to 72 h did not reveal immunoreactive bands despite the ability to immunoblot for α-tubulin. **d** Representative western blot for tau phosphorylated at S202 in rat cortical neurons (RCNs) did not reveal any changes in immunoreactivity for MCMV infected (Inf.) cultures, compared to mock infected (Mock) cells at 12 (left blot) and 48 (right blot) HPI

phosphatases (Rahman et al. 2006). There are numerous kinases that may target tau, and we chose to investigate one cellular kinase, glycogen synthase kinase 3 beta (GSK3β) that has been implicated in AD (Utton et al. 1997). GSK3β can phosphorylate tau at serine 396 and serine 202, as well as other sites (Utton et al. 1997; Liu et al. 2004), and was increased upon HSV-1 infection (Wozniak et al. 2009). We tested whether there was any change in steady state GSK3β protein levels during MCMV infection in our three cell types and found that the levels were not altered (Fig. 6). However, the virus could be modulating tau phosphorylation by affecting the activity of GSK3β, which might be reflected by the slightly slower migrating bands that were detected in the NIH3T3 lysates at 48 and 72 HPI (Fig. 6a). As we did not observe this for the B35 neuroblastoma cells or the RCNs (Fig. 6c), which have similar modifications, it is unlikely that GSK3β is involved.

To further address this, we used lithium chloride (LiCl) to inhibit GSK3 (targets both α and β isoforms; Noble et al. 2005) and analyzed levels of total tau and its phosphorylation at S396 and S202 in MCMV infected murine fibroblasts. Decreases in tau phosphorylation levels can be detected within four to 6 h after addition of LiCl (Lovestone et al. 1999). We treated cells with 50 mM LiCl and analyzed levels of total tau and tau phosphorylated at S396 and S202 in uninfected or infected fibroblasts at 48 HPI. In this case, if GSK3 were important for sites other than S396, we would expect to detect changes in the sizes of tau bands. We also included samples where uninfected and infected cells were given LiCl at 24 HPI instead of 0 HPI. LiCl has previously been reported to inhibit HSV and pseudorabies virus, but this was an early effect, with little impact if the LiCl was added after 13 h (Skinner et al. 1980; Ziaie et al. 1994). In case LiCl could also inhibit MCMV, we chose the latter treatment time (24 HPI, when the modifications of tau are largely just beginning) to give sufficient time for LiCl to prevent or reverse GSK3-mediated modifications (Lovestone et al. 1999). Consistent with the possible inhibition of MCMV, if LiCl was present throughout the

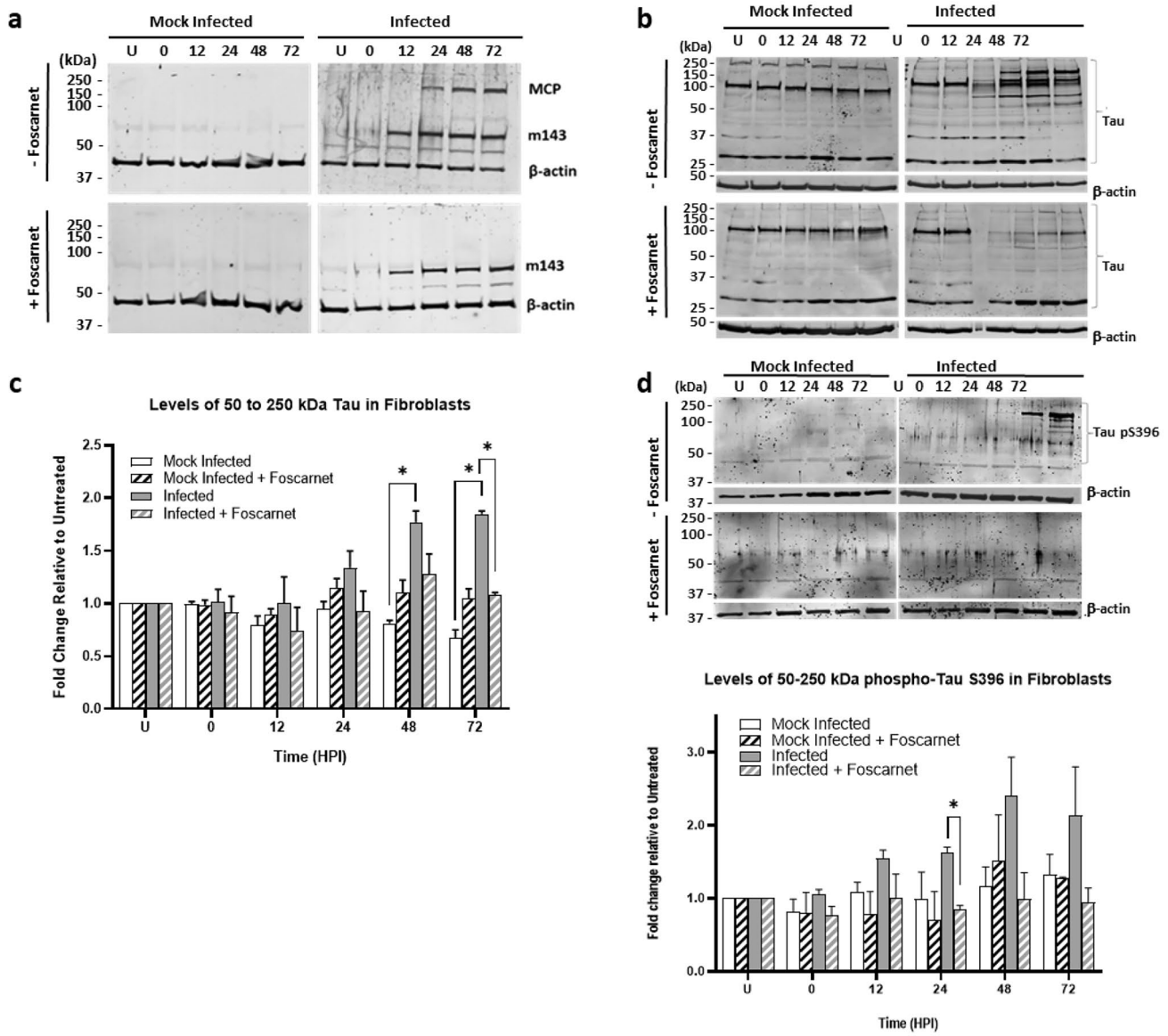

Fig. 5 Viral late gene products are required for tau increase. **a** Representative western blots for viral early protein m143 and viral late protein major capsid protein (MCP) from NIH3T3 fibroblasts either untreated (U), mock infected (left blots), or infected (right blots) with MCMV for 0 to 72 h post-infection (HPI) demonstrate successful MCMV infection (top blots). Treatment with the viral inhibitor foscarnet (lower blots) at the time of infection abolished the production of the late viral gene product MCP. **b** Representative western blots for total tau in NIH3T3 fibroblasts, untreated (U), mock infected (left blots), or infected with MCMV (right blots) for 0 to 72 h show that MCMV infection increased the levels of high molecular weight tau (upper blots) and treatment with foscarnet prevented this increase (lower blots). **c** Scanning densitometry of 50–250 kDa tau immunoreactive bands in samples from mock infected and infected fibroblasts either not treated or treated with foscarnet over 72 h show that viral inhibition prevented the increase in high molecular weight tau. **d** Representative western blots and scanning densitometry analysis of 50–250 kDa tau phosphorylated at serine 396 (S396) from the same samples used in Fig. 5b and c show that foscarnet inhibition of viral late gene product expression also prevented the increase in tau phosphorylation at S396. Data in **c** and **d** are expressed as means ± SD, normalized for equal loading against β-actin with the level for untreated (U) being set as 1.0. Significant differences between treatment groups are indicated by $*p \leq 0.05$, (two-way repeated measures ANOVA with Fisher's least significant difference (LSD) post hoc; $n = 3$)

48 h of infection, most of the changes in tau were absent (Fig. 7a–b), whereas delaying the addition of LiCl until 24 HPI did not reverse or prevent most of the increase in tau immunoreactive bands (Fig. 7a) and had only modest effects on the phosphorylation of tau at S396 (Fig. 7b). In neither treatment regimen did we detect altered banding patterns for S202 (Fig. 7c). Thus, these results are consistent with a possible early inhibition of MCMV by LiCl, and it appears that GSK3 does not play a major role in MCMV infection-mediated modifications of tau.

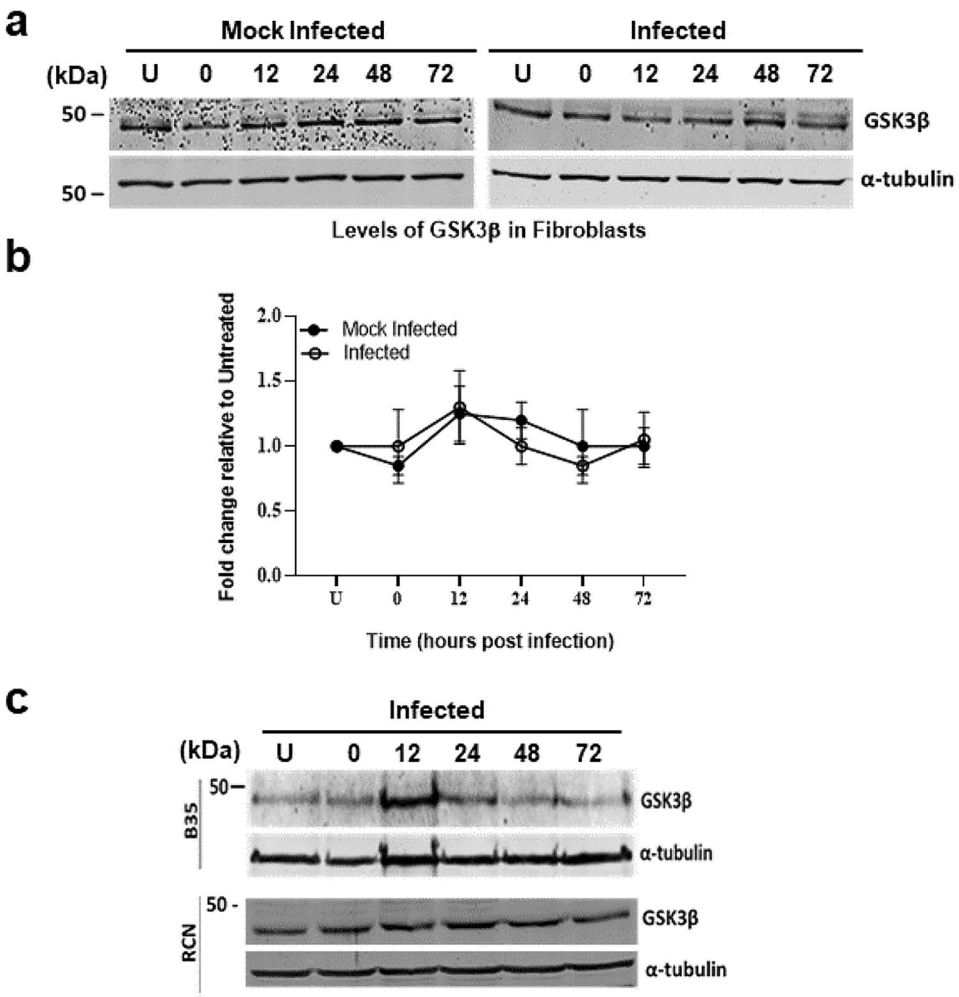

Fig. 6 MCMV infection does not affect levels of GSK3β. **a** Representative western blots and **b** densitometric analysis showing that the levels of GSK3β in untreated (U), mock infected, or murine cytomegalovirus (MCMV) infected fibroblasts from 0 to 72 h post-infection (HPI) are not affected by MCMV infection in NIH3T3 fibroblasts. Data are plotted as means ± SD, normalized for equal loading against α tubulin, with the level for 0 h set to 1.0 ($n = 3$). **c** Representative western blots showing levels of GSK3β does not change with MCMV infection in B35 neuroblastoma cells or rat cortical neurons (RCNs)

LiCl has been reported to inhibit HSV and pseudorabies virus, but not to our knowledge previously any beta or gamma herpesvirus (Skinner et al. 1980; Ziaie and Kefalides 1989; Ziaie et al. 1994). To investigate this possibility, we checked for expression of viral early E1 proteins and viral late MCP by western blotting, and titered infectious virus from conditioned media from all conditions (Fig. 8). When LiCl was present throughout the 48 h of infection, there was a reduction in all of the E1 isoforms, and MCP was below the limit of detection (Fig. 8a). The titer of infectious virus was decreased by 5 logs (Fig. 8b). Consistent with the reports for HSV that LiCl inhibits it at an early stage, when LiCl was added at 24 HPI, there was reduced but detectable MCP expression (Fig. 8a). However, the infectious virus production was still decreased by about a log compared to infected cells without LiCl treatment (Fig. 8b). Based on this, we inferred that LiCl is inhibitory to MCMV, probably at an early stage, like it is for HSV. The modest changes when the LiCl addition was delayed to 24 h prior to harvest support the hypothesis that GSK3 is unlikely to be involved in MCMV-mediated tau phosphorylation and other kinases must be considered for further investigation, such as the viral early/late kinase M97, or PKA, which was also upregulated in HSV-1 infected cells (Wozniak et al. 2009).

Discussion

Using MCMV infection in mouse and rat cells, we demonstrate that this can be a novel system to investigate early steps leading to changes in tau that are associated with increasing aggregation and Alzheimer's disease. MCMV is able to infect both mice and rats as permissive hosts (Smith et al. 1986). We have demonstrated that MCMV can undergo productive infection of rat neuronal models (B35 neuroblastoma cells and primary RCN) in vitro with kinetics of infection similar to mouse fibroblasts, although the delayed detection of MCP compared to CPE indicates a possibly slower replication in RCNs. An early morphological change seen in CMV-infected cells is multinucleated rounded cells that function as virus replication factories (Van Den Pol et al. 2000). All three cell types demonstrated a similar altered

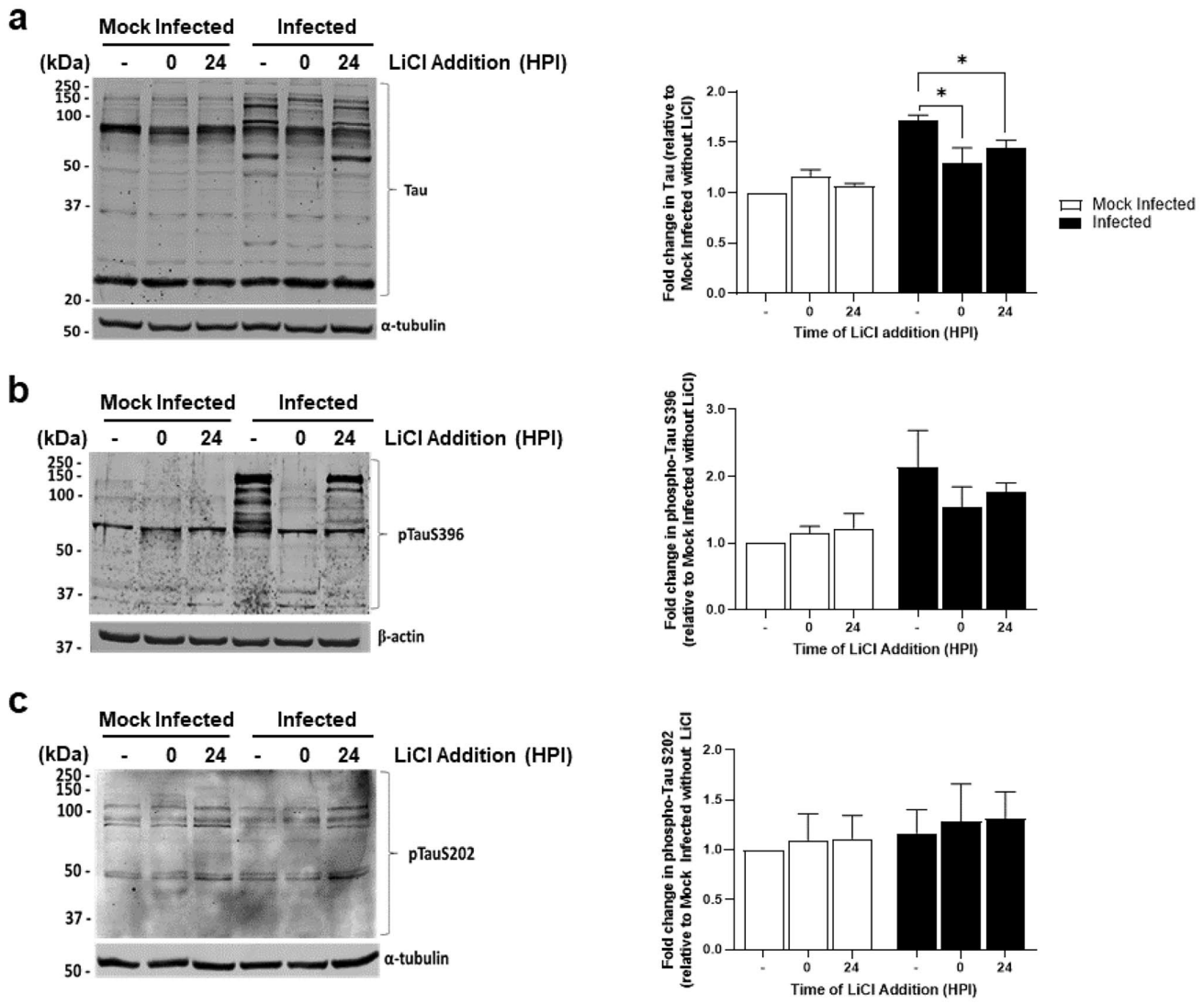

Fig. 7 Inhibition of GSK3 by LiCl minimally affects increase in tau and phosphorylation at S396 Representative western blots and graphs of densitometric analyses for total tau (**a**) or tau phosphorylated at S396 (**b**) or S202 (**c**) in untreated (U), mock infected, and murine cytomegalovirus (MCMV)-infected fibroblasts at 48 h post-infection (HPI) treated with 50 mM LiCl at either the time of infection (applied at the 0 h, 48 h of LiCl exposure) or 24 h later (24 h of LiCl exposure). Compared to MCMV infected cells not exposed to LiCl, LiCl exposure for the entire 48 h of infection or for the last 24 h of infection decreased the levels of total tau, but not its phosphorylation at either S396 or S202. Data are plotted as means ± SD, normalized for equal loading against β-actin, setting the level for 0 h at 1.0. Significant differences compared to 0 HPI at $p \leq 0.05$ are indicated by an asterisk (*; two-way repeated measures ANOVA and Fisher's least significant difference (LSD) post hoc test; $n = 3$)

morphology following MCMV infection at a dose of 2 PFU/cell as quantitated in NIH3T3 fibroblast cells. Expression of MCMV early protein E1 and late protein MCP in B35 neuroblastoma cells along with production of infectious virus at a titer similar to that seen from fibroblasts all confirmed successful completion of CMV replication. In the primary RCN, a similar cytopathic effect was observed and all 4 isoforms of E1 were detected. However, MCP was low but detectable at 72 h, but below the limit of detection at 48 h, consistent with the titer at 48 h that was 2 orders of magnitude lower, compared to the fibroblasts or B35 cells. It has been reported that neurons are not the most permissive cells for CMV or HSV infection (Van Den Pol et al. 2000; Cheeran et al. 2005; Braun et al. 2006; Sehrawat et al. 2018). Our data is consistent with these studies, in that the more differentiated neurons are less permissive. However, neuronal-type cells can clearly be infected by MCMV.

While changes in tau phosphorylation during HSV-1 infection have been studied (Wozniak et al. 2009; De Chiara et al. 2019; Powell-Doherty et al. 2020), we have not found similar published analyses for total tau. Because increased total tau levels have been fairly consistently detected in the

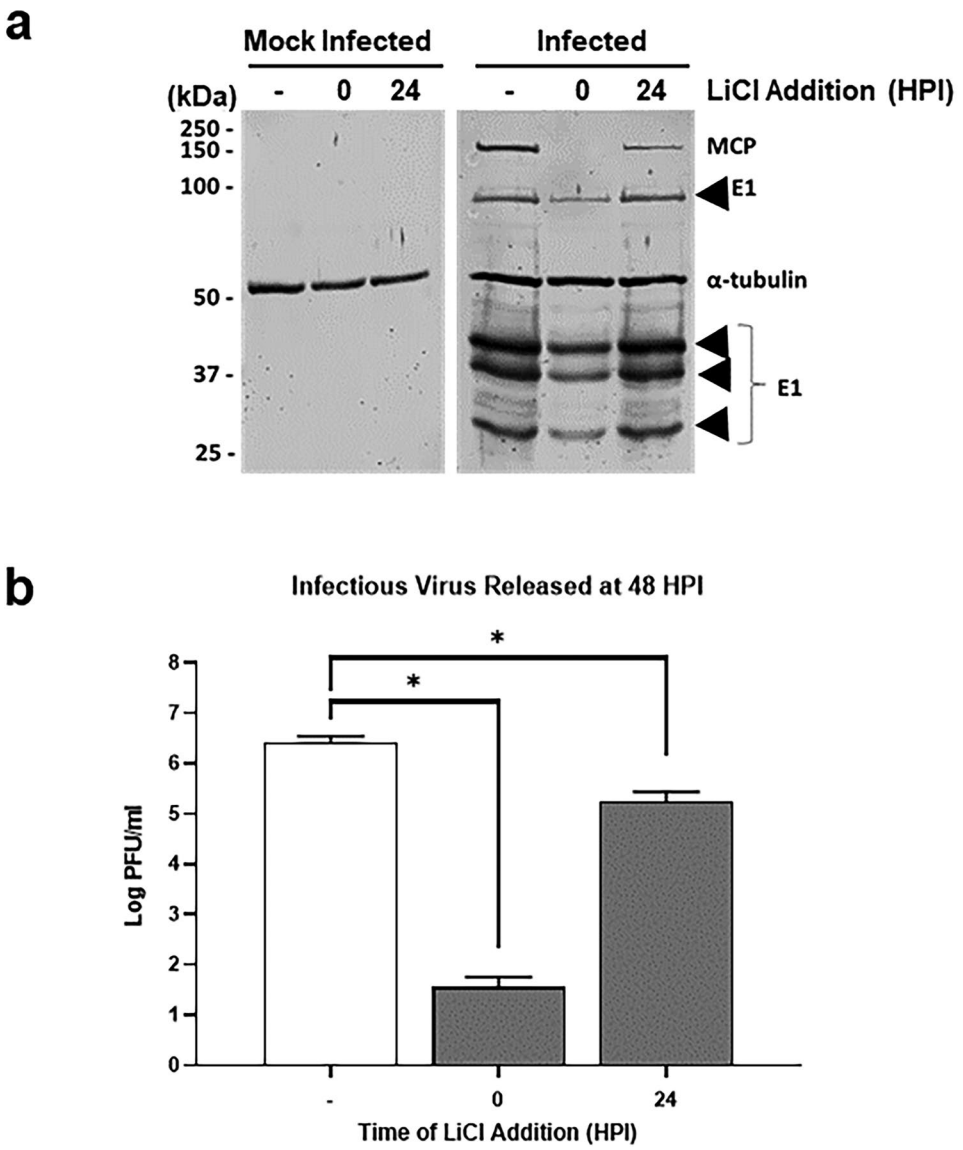

Fig. 8 Lithium chloride inhibits MCMV. **a** Representative western blots from NIH3T3 fibroblasts either mock infected (M) or infected with MCMV for 48 h and treated with 50 mM LiCl either for the entire 48 h of infection (added at the 0 h media change) or for the last 24 h of infection (added at 24 HPI) show that continuous exposure to LiCl during infection decreased expression of viral late major capsid protein (MCP), but had less effect on early (E1) proteins, while delaying treatment with LiCl for 24 h ameliorated the effect of LiCl on viral protein production. **b** Viral titers measured at 48 h post-infection (HPI) using a standard viral plaque assay were decreased by LiCl exposure during the entire time of infection (0), but were far less inhibited if LiCl treatment occurred 24 HPI (24). Data are plotted as means ± SD ($n = 3$). Significant differences compared to infected cultures not receiving LiCl are indicated by $*p \leq 0.05$ (one-way ANOVA with Fisher's least significant difference (LSD) post hoc)

cerebrospinal fluid of AD patients (reviewed in Hampel et al. 2010), and both intracellular tau levels and tau phosphorylation have been reported to have possible pathological effects for AD (Hu et al. 2016; Iqbal et al. 2016), it may be important to assess total tau, as well as tau modifications. We used a polyclonal antibody directed to the C-terminus of tau to visualize changes during CMV infection. Interestingly, some of the lower molecular weight forms of tau appeared to decrease with a concurrent increase in higher molecular weight forms after CMV infection. Only the increase in tau forms of over 50 kDa was significantly different compared to uninfected cells. This may reflect altered post-translational modifications of specific isoforms. Recent studies have presented evidence for current antivirals preventing induced tau hyperphosphorylation in HSV-1 infected cells (Wozniak et al. 2011; Powell-Doherty et al. 2020). We used foscarnet, an FDA-approved antiviral, to test whether this held true for CMV infected cells. The levels of high-molecular weight tau forms were no longer increased in the presence of foscarnet, nor did we see the increased phosphorylation at Ser396. Although we did not analyze individual bands, there are some changes which may be of interest. Infection increased a protein migrating around 75 kDa from 12 HPI in infected cells. The presence of this band remains in foscarnet treated cultures (Fig. 4). Thus, although the majority of the changes were dependent on late gene expression, early gene products may also lead to some alterations in tau. This could be important for treatment paradigms proposing to use current antivirals in AD patients, since most of the current therapies inhibit genome replication, retaining early gene expression. In addition, Powell-Doherty et al. (2020) reported an increase in tau phosphorylated at S396 with acylovir treatment alone, which they pointed out might be concerning for anti-AD therapy. We did not detect any such increases due to foscarnet alone.

Changes in tau phosphorylation specific to AD during HSV-1 infection have been studied, including some western blot analyses (Wozniak et al. 2009, De Chiara et al. 2019; Powell-Doherty et al. 2020). Although total levels of tau phosphorylation at certain specific sites increased, it is not clear how much was in high molecular weight forms of tau as Wozniak et al. (2009) did not do western blot analysis, and the blots shown in De Chiara et al. (2019) or Powell-Doherty et al. (2020) generally had a maximum molecular weight of 75 kDa. We have shown that phosphorylation of tau at serine 396 is enhanced during MCMV infection and the hyperphosphorylated tau forms migrate between 75 and 250 kDa (Fig. 3); the size range for most increased total tau forms (Fig. 2). This result is similar to a study on physiological tau from cerebrospinal fluid of patients that had different dementias, including AD-specific dementia (Sjogren et al. 2001). These authors published that the higher migrating tau forms were mostly hyperphosphorylated (as opposed to having other types of post-translational modifications) and were detected by antibodies specific for total as well as phosphorylated tau. We showed that slower migrating phospho-tau forms were detected starting at 24 HPI which were enhanced at 48 HPI and 72 HPI in fibroblasts and neurons. Based on this evidence, we propose that viral late proteins may be involved in inducing phosphorylation of tau, including at serine 396, by similar mechanisms in these two cell types.

For B35 neuroblastoma cells, there were more phospho-tau forms detected in uninfected cells as compared to fibroblasts and primary neurons. This was not surprising given that tumor cells often have a higher level of global phosphorylation (Lee et al. 2016). A possible decrease in intensity of all forms of tau was seen at 12 and 24 HPI, which could be due to a global downregulation of phosphorylation by CMV infection, although more studies are needed to evaluate this. CMV is known to incorporate host phosphatases in its virion, which are released into the host cell upon infection (Hakki and Geballe 2008). However, enhancement of phospho-tau forms at ~ 150 kDa was still detected during CMV infection of B35 cells at later times points. Given the amount of increase in size of tau immunoreactive bands, it is highly unlikely that the changes are solely due to phosphorylation at one site, indicating that other sites on tau may be significantly modified by phosphorylation or other modifications in all three cell types we tested.

Phosphorylation of tau at serine 202 was also shown to be increased in HSV-1 infected human neuroblastomas (Wozniak et al. 2009). In rat B35 neuroblastoma cells, there was no detectable phosphorylation at serine 202 with or without CMV infection. In mouse fibroblasts and primary neurons, the levels did not change with MCMV infection. Based on this evidence, we concluded that MCMV infection does not affect phosphorylation at serine 202 of tau in our cell culture models. MCMV infection, thus, selectively upregulates phosphorylation at a key site involved in AD pathology (i.e., serine 396). This may be due to CMV affecting specific kinase levels or activity. In studies using mutated phosphorylation sites, it was consistently found that phosphomimetic mutations at S396 promote aggregation and/or decrease association with the microtubules, while similar mutations at S202 did not have this effect (Abraha et al 2000; Haase et al. 2004; Ding et al. 2006). In addition, in mouse cultured brain slice models, S396 phosphorylation was particularly noted at plaque sites, which was not true for other phosphorylation sites tested in that study (Foidl and Humpel 2018). Identifying the mechanisms involved in CMV-mediated tau hyperphosphorylation may be important for finding therapies to target relevant pathways.

HSV-1 infection leads to increased levels of GSK3β and protein kinase A (PKA; Wozniak et al. 2009). GSK3β is one of several kinases that can phosphorylate tau at both serine 202 and serine 396 (Utton et al. 1997; Liu et al. 2004). We did not find any evidence for a change in GSK3β levels during MCMV infection, although there did appear to be a slightly slower migrating band that was more pronounced in infected fibroblasts. However, as this was not observed in either the B35 neuroblastoma cells or the primary cortical neurons, it is unlikely that it is required for the observed modifications of tau. When we inhibited GSK3 activity by using lithium chloride, we found that under conditions when the virus was minimally inhibited, the changes in tau were largely retained. Thus, with no changes in GSK3β levels, the differential effect on S202 and S396, and the minimal effect of LiCl, it is likely that other kinases are more important for the tau modifications in the context of MCMV infection. The combination of late gene requirements and changes in phosphorylation raises the intriguing possibility that the viral kinase, M97 (UL97 homologue) could play a role in phosphorylation of tau, as the mRNA is highly upregulated at late times (Rawlinson et al. 1997). When Wagner et al. (2000) did kinase assays on cells using an M97 deletion mutant, they did observe loss of some bands in the lower molecular weight ranges. However, several bands in the 50 to 100 kDa range were evident in fibroblast samples infected with both the wild-type virus and virus deleted of m97. Although the blots shown in the Wagner et al. paper did not include forms above 100 kDa, these results support that viral infection leads to phosphorylation changes which are not solely related to M97, but a role in tau phosphorylation cannot be ruled out. In addition to the up-regulation of PKA by HSV-1 reported by Wozniak et al. (2009), and of p38 MAPK by MCMV (Tang-Feldman et al. 2013), alterations in phosphorylation of a variety of kinases has been reported in HCMV infected cells (Coute et al. 2020). Several of these are also tau kinases reported to be active in Alzheimer's disease brains (Martin et al. 2013), such as PKA, protein kinase C, casein kinase II, and p38 MAPK. Identification of the kinase(s) involved in the tau phosphorylation following MCMV infection remains to be determined, however these are attractive candidates.

Lithium chloride can inhibit alpha herpesvirus replication (Skinner et al. 1980, Ziaie and Kefalides 1989, Ziaie et al. 1994), so it is not surprising that it can also inhibit beta herpesviruses like MCMV. This may reflect a requirement for GSK3 activity during early stages of herpesvirus infection or LiCl may affect the virus replication through some other mechanism unrelated to GSK3. The impact of LiCl on herpesviruses is intriguing in light of reports that people on long-term lithium therapy had reduced risk of AD compared to those on other mood stabilizers (Nunes et al. 2007), and a small follow-up trial which supported that lithium could be beneficial in some patients with mild cognitive impairment (Forlenza et al. 2011). Further analysis on the infection status of AD patients, whether they benefitted from treatment with lithium chloride, and studies on the mechanism of lithium inhibition of herpesviruses may be useful both to determine the possible role of GSK3 or other functions of lithium (Pan et al. 2018) and find new ways to control herpes virus infections.

We have shown here that MCMV is capable of inducing alterations of tau similar to those associated with AD. These mainly require viral late gene products, and are largely preventable with antiviral drugs. Unlike animal models of HSV (Webre et al. 2012; Sehrawat et al. 2018), MCMV can be used in its natural murine host and compared with the closely related permissive rat. A clinical trial is currently underway to test anti-HSV drugs in patients with AD-related dementias (Devanand 2019). While this is hugely encouraging, mechanistic studies are ultimately needed to characterize virus-host interactions for sustainable treatment or preventives and hopefully to develop a better understanding of early steps, direct and indirect viral effects including immune roles (Canivet et al. 2019; De Chiara et al. 2019), which may lead to better diagnostics before dementias develop, or improved interventions for different possible triggers and pathways of AD.

Funding P. H. Mody received research grant from the Texas Woman's University Center for Student Development $500.

Data availability All data supporting the findings are available within the paper. Raw data, calculations, and additional blot images are available from the authors upon request.

Declarations

Conflict of interest The authors declare no competing interests.

References

Abraha A, Ghoshal N, Gamblin TC, Cryns V, Berry RW, Kuret J, Binder LI (2000) C-terminal inhibition of tau assembly in vitro and in Alzheimer's disease. J Cell Sci 113:3737–3745. https://doi.org/10.1242/jcs.113.21.3737

Alonso AD, Di Clerico J, Li B, Corbo CP, Alaniz ME, Grundke-Iqbal I, Iqbal K (2010) Phosphorylation of tau at Thr212, Thr231, and Ser262 combined causes neurodegeneration. J Biol Chem 285:30851–30860. https://doi.org/10.1074/jbc.M110.110957

Ando K, Maruko-Otake A, Ohtake Y, Hayashishita M, Sekiya M, Iijima KM (2016) Stabilization of microtubule-unbound tau via tau phosphorylation at Ser262/356 by Par-1/MARK contributes to augmentation of AD-related phosphorylation and Abeta42-induced tau toxicity. PLoS Genet 12:e1005917. https://doi.org/10.1371/journal.pgen.1005917

Avila J, Lucas JJ, Perez M, Hernandez F (2004) Role of tau protein in both physiological and pathological conditions. Physiol Rev 84:361–384. https://doi.org/10.1152/physrev.00024.2003

Barnes LL, Capuano AW, Aiello AE, Turner AD, Yolken RH, Torrey EF, Bennett DA (2015) Cytomegalovirus infection and risk of Alzheimer disease in older black and white individuals. J Infect Dis 211:230–237. https://doi.org/10.1093/infdis/jiu437

Boban M, Leko MB, Miskic T, Hof PR, Simic G (2019) Human neuroblastoma SH-SY5Y cells treated with okadaic acid express phosphorylated high molecular weight tau-immunoreactive protein species. J Neurosci Methods 319:60–68. https://doi.org/10.1016/j.jneumeth.2018.09,030

Braun E, Zimmerman T, Hur TB, Reinhartz E, Fellig Y, Panet A, Steiner I (2006) Neurotropism of herpes simplex virus type 1 in brain organ cultures. J Gen Virol 87:2827–2837. https://doi.org/10.1099/vir.0.81850-0

Bloom GS (2014) Amyloid-β and tau: The trigger and bullet in Alzheimer disease pathogenesis. JAMA Neurol 71(4):505–508. https://doi.org/10.1001/jamaneurol.2013.5847

Buee L (2000) Tau protein isoforms, phosphorylation and role in neurodegenerative disorders. Brain Res Rev 33:95–130

Canivet C, Uyar O, Rheaume C, Piret J, Boivin G (2019) The recruitment of peripheral blood leukocytes to the brain is delayed in susceptible BALB/c compared to resistant C57BL/6 mice during herpes simplex virus encephalitis. J Neurovirol 25:372–383. https://doi.org/10.1007/s13365-019-00730-5. Epub 2019 Feb. 13

Carlyle BC, Nairn AC, Wang M, Yang Y, Jin LE, Simen AA, Ramos BP, Bordner KA, Craft GE, Davies P, Pletikos M, Sestan N, Arnsten AF, Paspalas CD (2014) cAMP-PKA phosphorylation of tau confers risk for degeneration in aging association cortex. Proc Natl Acad Sci USA 111:5036–5041. https://doi.org/10.1073/pnas.1322360111

Cheeran MC, Hu S, Ni HT, Sheng W, Palmquist JM, Peterson PK, Lokensgard JR (2005) Neural precursor cell susceptibility to human cytomegalovirus diverges along glial or neuronal differentiation pathways. J Neurosci Res 82:839–850. https://doi.org/10.1002/jnr.20682

Cheeran MC, Lokensgard JR, Schleiss MR (2009) Neuropathogenesis of congenital cytomegalovirus infection: disease mechanisms and prospects for intervention. Clin Microbiol Rev 22:99–126. https://doi.org/10.1128/CMR.00023-08

Ciocco-Schmitt GM, Karabekian Z, Godfrey EW, Stenberg RM, Campbell AE, Kerry JA (2002) Identification and characterization of novel murine cytomegalovirus M112–113 (e1) gene products. Virology 294:199–208. https://doi.org/10.1006/viro.2001.1311

Coute Y, Kraut A, Zimmermann C, Buscher NH, A-M, Bruley, C., De Andrea, M. Wangen, C. Hahn, F., Marschall, M. Plachter, B. (2020) Mass spectrometry-based characterization of the virion proteome, phosphoproteome, and associated kinase activity of human cytomegalovirus. Microorgnaisms 8:820. https://doi.org/10.3390/microorganisms8060820

Crumpacker CS (1992) Mechanism of action of foscarnet against viral polymerases. Am J Med 92:3S-7S. https://doi.org/10.1016/0002-9343(92)90329-a

De Chiara G, Piacentini R, Fabiani M, Mastrodonato A, Marcocci ME, Limongi D, Napoletani G, Protto V, Coluccio P, Celestino I, Li Puma DD, Grassi C, Palamara AT (2019) Recurrent herpes

simplex virus-1 infection induces hallmarks of neurodegeneration and cognitive deficits in mice. PLoS Pathog 15:e1007617. https://doi.org/10.1371/journal.ppat.1007617

Devanand D (2019) Anti-viral therapy in Alzheimer's disease. Available via NIH U.S. National Library of Medicine. https://clinicaltrials.gov/ct2/show/NCT0328916. Accessed 7 Aug 2019

Ding H, Matthews TA, Johnson GV (2006) Site-specific phosphorylation and caspase cleavage differentially impact tau-microtubule interactions and tau aggregation. J Biol Chem 281:19107–19114. https://doi.org/10.1074/jbc.M511697200

Foidl, BM, Humpel C (2018) Differential Hyperphosphorylation of Tau-S199, -T231, and -S396 in organotypic brain slices of Alzheimer mice. a model to study early tau hyperphosphorylation using okadaic acid. Front Aging Neurosci 10:113. https://doi.org/10.3389/fnagi.2018.00113

Forlenza OV, Diniz BS, Radanovic M, Santos FS, Talib LL, Gattaz WF (2011) Disease-modifying properties of long-term lithium treatment for amnestic mild cognitive impairment: randomised controlled trial. Br J Psychiat 198:351–356. https://doi.org/10.1192/bjp.bp.110.080044

Haase C, Stieler JT, Arendt T, Holzer M (2004) Pseudophosphorylation of tau protein alters its ability for self-aggregation. J Neurochem 88:1509–1520. https://doi.org/10.1046/j.1471-4159.2003.02287.x

Hakki M, Geballe AP (2008) Cellular serine/threonine phosphatase activity during human cytomegalovirus infection. Virology 380:255–263. https://doi.org/10.1016/j.virol.2008.07.028

Hampel H, Blennow K, Shaw LM, Hoessler YC, Zetterberg H, Trojanowski JQ (2010) Total and phosphorylated tau protein as biological markers for Alzheimer's disease. Exp Gerontol 45:30–40. https://doi.org/10.1016/J.exger.2009.10.010

Hanson LK, Slater JS, Karabekian Z, Virgin HWT, Biron CA, Ruzek MC, van Rooijen N, Ciavarra RP, Stenberg RM, Campbell AE, (1999) Replication of murine cytomegalovirus in differentiated macrophages as a determinant of viral pathogenesis. J Virol 73:5970–5980. https://doi.org/10.1128/jvi.73.7.5970-5980.1999

Hanson LK, Dalton BL, Cageao LF, Brock RE, Slater JS, Kerry JA, Campbell AE (2005) Characterization and regulation of essential murine cytomegalovirus genes m142 and m143. Virology 334:166–177. https://doi.org/10.1016/j.virol.2005.01.046

Hanson LK, Slater JS, Cavanaugh VJ, Newcomb WW, Bolin LL, Nelson CN, Fetters LD, Tang Q, Brown JC, Maul GG, Campbell AE (2009) Murine cytomegalovirus capsid assembly is dependent on US22 family gene M140 in infected mactrophages. J Virol 83:7449–7456. https://doi.org/10.1128/JVL00325-09

Hogestyn JM, Mock DJ, Mayer-Proschel M (2018) Contributions of neurotropic human herpes viruses herpes simplex virus 1 and human herpesvirus 6 to neurodegenerative disease pathology. Neural Regen Res 13:211–221. https://doi.org/10.4103/1673-5374.226380

Hu Y, Li XC, Wang ZH, Zhang X, Liu XP, Feng Q, Wang Q, Yue Z, Chen Z, Ye K, Wang JZ, Liu GP (2016) Tau accumulation impairs mitophagy via increasing mitochondrial membrane potential and reducing mitochondrial Parkin. Oncotarget 7:17356–17368. https://doi.org/10.18632/oncotarget.7861

Iqbal K, Liu F, Gong CX (2016) Tau and neurodegenerative disease: the story so far. Nat Rev Neurol 12:15–27. https://doi.org/10.1038/nrneurol.2015.225

Jackson SE, Redeker A, Arens R, van Baarle D, van den Berg SPH, Benedict CA, Čičin-Šain L, Hill AB, Wills MR (2017) CMV immune evasion and manipulation of the immune system with aging. Geroscience 39:273–291. https://doi.org/10.1007/s11357-017-9986-6

Johnson GVW, Stoothoff WH (2004) Tau phosphorylation in neuronal cell function and dysfunction. J Cell Sci 117:5732–5739. https://doi.org/10.1242/jcs.01558

Kammerman EM, Neumann DM, Ball MJ, Lukiw W, Hill JM (2006) Senile plaques in Alzheimer's diseased brains: possible association of beta-amyloid with herpes simplex virus type 1 (HSV-1) L-particles. Med Hypotheses 66(2):294–299. https://doi.org/10.1016/j.mehy.2005.07.033

Kimura T, Ono T, Takamatsu J, Yamamoto H, Ikegami K, Kondo A, Hasegawa M, Ihara Y, Miyamoto E, Miyakawa T (1996) Sequential changes of tau-site-specific phosphorylation during development of paired helical filaments. Dementia 7(4):177–181

Kovacs GG (2017) Tauopathies. Handb Clin Neurol 145:355–368. https://doi.org/10.1016/B978-0-12-802395-2.00025-0

La Joie, R. Visani, AV, Baker, SL, Brown, JA, Bourakova, V, Cha, J, Chaudhary, K, Edward, L, Iaccarino, L, Janabi, M, Lesman-Segev, OH, Miller, ZA, Perry, DC, O'Neil, JP, Pham, J, Rojas, JC, Rosen, HJ, Seeley, WW, Tsai, RM, Miller, BL, Jagust, WJ, Rabinovici, GD (2020) Prospective longitudinal atrophy in Alzheimer's disease correlates with the intensity and topography of baseline tau-PET. Sci Transl Med 12(5240):eaau5732. https://doi.org/10.1126/scitranslmed.aau5732

Lee J, Ahn E, Park WK, Park S (2016) Phosphoproteome profiling of SH-SY5y neuroblastoma cells treated with anesthetics: sevoflurane and isoflurane affect the phosphorylation of proteins involved in cytoskeletal regulation. PLoS ONE 11(9):e0162214. https://doi.org/10.1371/journal.pone.0162214

Letenneur L, Peres K, Fleury H, Garrigue I, Barberger-Gateau P, Helmer C, Orgogozo J-M, Gauthier S, Dartigues J-F (2008) Seropositivity to herpes simplex virus antibodies and risk of Alzheimer's disease: a population-based cohort study. PlosOne 3(11):e3637. https://doi.org/10.1371/journal.pone.0003637

Lin WR, Wozniak MA, Cooper RJ, Wilcock GK, Itzhaki RF (2002) Herpesviruses in brain and Alzheimer's disease. J Pathol 197(3):395–402. https://doi.org/10.1002/path.1127

Liu SJ, Zhang JY, Li HL, Fang ZY, Wang Q, Deng HM, Gong CX, Grundke-Iqbal I, Iqbal K, Wang JZ (2004) Tau becomes a more favorable substrate for GSK-3 when it is prephosphorylated by PKA in rat brain. J Biol Chem 279(48):50078–50088. https://doi.org/10.1074/jbc.M406109200

Lovestone S, David DR, Webster M-T, Kaech S, Brion J-P, Matus A, Anderton BH (1999) Lithium reduces tau phosphorylation: effects in living cells and in neurons at therapeutic concentrations. Biol Phsychiatry 45:995–1003. https://doi.org/10.1015/s0006-3223(98)00183-8

Lurain NS, Hanson BA, Martinson J, Leurgans SE, Landay AL, Bennett DA, Schneider JA (2013) Virological and immunological characteristics of human cytomegalovirus infection associated with Alzheimer disease. J Infect Dis 208(4):564–572. https://doi.org/10.1093/infdis/jit210

Manicklal S, Emery VC, Lazzarotto T, Boppana SB, Gupta RK (2013) The "silent" global burden of congenital cytomegalovirus. Clin Microbiol Rev 26(1):86–102. https://doi.org/10.1128/CMR.00062-12

Martin L, Latypova X, Wilson CM, Magnaudeix A, Perrin M-L, Yardin C, Terro F (2013) Tau protein kinases: involvement in Alzheimer's disease. Ageing Res Rev 12:289–309. https://doi.org/10.1016/j.arr.2012.06.003

McQuillan G, Kruszon-Moran D, Flagg E, Paulose-Ram R (2018) Prevalence of herpes simplex virus type 1 and type 2 in persons aged 14–49: United States, 2015–2016. NCHS Data Brief Feb (304):1–8

NIA (2018) Alzheimer's disease fact sheet. Available via National Institute of Health. https://www.nia.nih.gov/health/alzheimers-disease-fact-sheet. Accessed 7 Aug 2019

Noble W, Planel E, Zehr C, Olm V, Meyerson J, Suleman F, Gaynor K, Wang L, LaFrancois J, Feinstein B, Burns M, Krishnamurthy P, Wen Y, Bhat R, Lewis J, Dickson D, Duff K (2005) Inhibition of glycogen synthase kinase-3 by lithium correlates with reduced tauopathy and degeneration in vivo. Proc Natl Acad Sci USA 102(19):6990–6995. https://doi.org/10.1073/pnas.0500466102

Nunes PV, Forlenza OV, Gattaz WF (2007) Lithium and risk for Alzheimer's disease in elderly patients with bipolar disorder. Br J Psychiat 190:359–360. https://doi.org/10.1192/bjp.bp.106.029868

Otey CA, Boukhelifa M, Maness P (2003) B35 neuroblastoma cells: an easily transfected, cultured cell model of central nervous system neurons. Methods Cell Biol 71:287–304. https://doi.org/10.1016/s0091-679x(03)01013-6

Pan Y, Short JL, Newman SA, Choy KHC, Tiwari D, Yap C, Senyschyn D, Banks WA, Nicolazzo JA (2018) Cognitive benefits of lithium chloride in APP/PS1 mice are associated with enhanced brain clearance of β-amyloid. Brain Behav Immun 70:36–47. https://doi.org/10.1016/j.bbi.2018.03.007

Powell-Doherty RD, Abbott ARN, Nelson LA, Bertke AS (2020) Amyloid-β and p-tau anti-threat response to herpes simplex virus 1 infection in primary adult murine hippocampal neurons. J Virol 94(9):e01874-e1919. https://doi.org/10.1128/JVI.01874-19

Rahman A, Grundke-Iqbal I, Iqbal K (2006) PP2B isolated from human brain preferentially dephosphorylates ser-262 and ser-396 of the Alzheimer disease abnormally hyperphosphorylated tau. J Neural Transm 113(2):219–230. https://doi.org/10.1007/s00702-005-0313-5

Rawlinson WD, Zeng F, Farrell HE, Cunningham AL, Scalzo AA, Booth TWM, Scott GM (1997) The murine cytomegalovirus (MCMV) homolog of the HCMV phosphotransferase (UL97 (9pk)) gene. Virol 233:358–363. https://doi.org/10.1006/viro.1997.8593

Readhead B, Haure-Mirande JV, Funk CC, Richards MA, Shannon P, Haroutunian V, Sano M, Liang WS, Beckmann ND, Price ND, Reiman EM, Schadt EE, Ehrlich ME, Gandy S, Dudley JT (2018) Multiscale analysis of independent Alzheimer's cohorts finds disruption of molecular, genetic, and clinical networks by human herpesvirus. Neuron 99(1):64-82.e7. https://doi.org/10.1016/j.neuron.2018.05.023

Sehrawat S, Kumar D, Rouse BT (2018) Herpesviruses: harmonious pathogens but relevant cofactors in other diseases? Front Cell Infect Microbiol 8:177. https://doi.org/10.3389/fcimb.2018.00177

Seifert JL, Som S, Hynds DL (2009) Differential activation of Rac1 and RhoA in neuroblastoma cell fractions. Neurosci Lett 450(2):176–180. https://doi.org/10.1016/j.neulet.2008.11.025

Shipley SJ, Parkin ET, Itzhaki RF, Dobson CB (2005) Herpes simplex virus interferes with amyloid precursor protein processing. BMC Microbiol 5:48. https://doi.org/10.1186/1471-2180-5-48

Sjogren M, Davidsson P, Tullberg M, Minthon L, Wallin A, Wikkelso C, Granerus AK, Vanderstichele H, Vanmechelen E, Blennow K (2001) Both total and phosphorylated tau are increased in Alzheimer's disease. J Neurol Neurosurg Psychiatry 70(5):624–630. https://doi.org/10.1136/jnnp.70.5.624

Skinner GR, Hartley C, Buchan A, Harper L, Gallimore P (1980) The effect of lithium chloride on the replication of herpes simplex virus. Med Microbiol Immunol 168(2):139–148. https://doi.org/10.1007/BF02121762

Smith CB, Wei LS, Griffiths M (1986) Mouse cytomegalovirus is infectious for rats and alters lymphocyte subsets and spleen cell proliferation. Arch Virol 90(3–4):313–323

Tang-Feldman YJ, Lockhead SR, Lochhead GR, Yu C, George M, Villablanca AC, Pomeroy CJ (2013) Murine cytomegalovirus (MCMV) infection upregulates p38 MAP kinase in aortas of Apo E KO mice: a molecular mechanism for MCMV-induced acceleration of atherosclerosis. Cardiovasc Transl Res 6:54–64. https://doi.org/10.1007/s12265-012-9428-x

Tzeng NS, Chung CH, Lin FH, Chinag CP, Yeh CB, Huang SY, Lu RB, Chang HA, Kao YC, Yeh HW, Chiang WS, Chou YC, Tsao CH, Wi YF, Chien WC (2018) Anti-herpetic medications and reduced risk of dementia in patients with herpes simplex virus infections—a nationwide, population-based cohort study in Taiwan. Neurotherapeutics 15:417–429. https://doi.org/10.1007/s13311-018-0611-x

Utton MA, Vandecandelaere A, Wagner U, Reynolds CH, Gibb GM, Miller CC, Bayley PM, Anderton BH (1997) Phosphorylation of tau by glycogen synthase kinase 3 beta affects the ability of tau to promote microtubule self-assembly. Biochem J 323(Pt 3):741–747. https://doi.org/10.1042/bj3230741

Van Den Pol AN, Vieira J, Spencer DD, Santarelli JG (2000) Mouse cytomegalovirus in developing brain tissue: analysis of 11 species with GFP-expressing recombinant virus. J Comp Neurol 427(4):559–580. https://doi.org/10.1002/1096-9861(20001127)427:4%3c559::aid-cne5%3e3.0.co;2-4

Wagner M, Michel D, Schaarschmidt P, Vaida B, Jonjic S, Messerle M, Mertens T, Koszinowski U (2000) Comparison between human cytomegalovirus pUL97 and murine cytomegalovirus (MCMV) pM97 expressed by MCMV and Vaccinia virus: pM97 does not confer ganciclovir sensitivity. J Virol 74:10729–10736. https://doi.org/10.1128/jvi.74.22.10729-10736.2000

Webre JM, Hill JM, Nolan NM, Clement C, McFerrin HE, Bhattacharjee PS, Hsia V, Neumann DM, Foster TP, Lukiw WJ, Thompson HW (2012) Rabbit and mouse models of HSV-1 latency, reactivation, and recurrent eye diseases. J Biomed Biotech. https://doi.org/10.1155/2012/612316

Wozniak MA, Frost AL, Itzhaki RF (2009) Alzheimer's disease-specific tau phosphorylation is induced by herpes simplex type 1. J Alzheimers Dis 16(2):341–350. https://doi.org/10.3233/JAD-2009-0963

Wozniak MA, Frost AL, Preston CM, Itzhaki RF (2011) Antivirals reduce the formation of key Alzheimer's disease molecules in cell cultures acutely infected with herpes simplex virus type 1. PLoS ONE 6(10):e25152. https://doi.org/10.1371/journal.pone.0025152

Ziaie Z, Brinker JM, Kefalides NA (1994) Lithium chloride suppresses the synthesis of messenger RNA for infected cell protein-4 and viral deoxyribonucleic acid polymerase in herpes simplex virus-1 infected endothelial cells. Lab Invest 70(1):29–38

Ziaie Z, Kefalides NA (1989) Lithium chloride restores host protein synthesis in herpes simplex virus-infected endothelial cells. Biochem Biophys Res Commun 160(3):1073–1078. https://doi.org/10.1016/s0006-291x(89)80112-3